RSC Advances

ROYAL SOCIETY OF CHEMISTRY

www.rsc.org/advances

Graphic Abstract

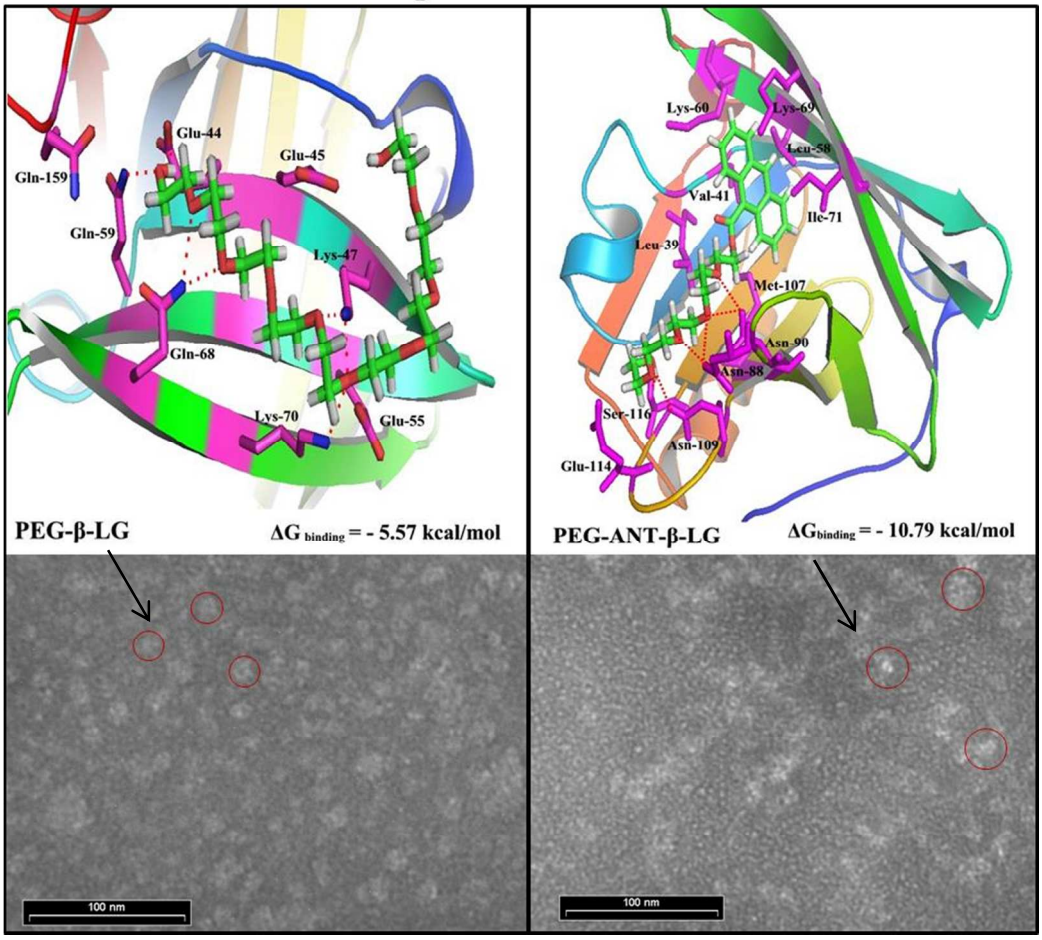

Revised RA-ART-04-2014-003303 for RSC Advances

Microscopic and thermodynamic analysis of PEG-*β*-lactoglobulin interaction

L. Bekale, P. Chanphai, S. Sanyakamdhorn, D. Agudelo and H. A. Tajmir-Riahi*

Department of Chemistry-Physics, University of Québec at Trois-Rivières, C. P. 500, Trois-Rivières (Québec), G9A 5H7, Canada

Key words: PEG, nanoparticles, polymer, beta-lactoglobulin, binding site, FTIR, CD, fluorescence, TEM, modeling

Abbreviations: PEG, poly(ethylene glycol); mPEG-anthracene, methoxypoly (ethylene glycol) anthracene; *β*-LG, beta-lactoglobulin; FTIR, Fourier transform infrared; CD, circular dichroism; TEM, transmission electron microscopy

*** Corresponding author: heidar-ali.tajmir-riahi@uqtr.ca :Tel: 819-376-5011 (3326)**

Abstract

We report the binding of milk *β*-lactoglobulin (*β*-LG) with PEG-3000, PEG-6000 and methoxypoly (ethylene glycol) anthracene (mPEG-anthracene) in aqueous solution at pH 7.4, using multiple spectroscopic methods, thermodynamic analysis, transmission electron microscopy (TEM) and molecular modeling. Thermodynamic and spectroscopic analysis showed that polymers bind *β*-LG *via* Van der Waals, H-bonding and hydrophobic interactions with overall binding constants $K_{\text{PEG-3000-}\beta\text{-LG}}$= 9.2 (± 0.9) x 10^3 M^{-1}, $K_{\text{PEG-6000-}\beta\text{-LG}}$= 9.7 (± 0.7) x 10^3 M^{-1} and $K_{\text{mPEG-anthracene-}\beta\text{-LG}}$= 5.5 (± 0.5) x 10^4 M^{-1}. The binding affinity was mPEG-antracene > PEG-6000 >PEG-3000. Transmission electron microscopy showed significant changes in protein morphology as polymer-protein complexation occurred with major increase in the diameter of the protein aggregate. Modeling showed several H-bonding systems between PEG and different amino acids stabilized polymer-*β*-LG complexes and the free binding energy indicated that the interaction process is spontaneous at room temperature. Furthermore, mPEG-anthracene is a stronger protein binder than PEG-3000 and PEG-6000 due to its major hydrophobic character.

Introduction

Polyethylene glycol (PEG) (scheme 1) is a non-ionic hydrophilic polymer with stealth behavior often used to increase the stability of particles and proteins in physiological conditions. PEG conjugation to therapeutic proteins has emerged as an effective strategy for drug-delivery.[1-5] PEGylation of peptide and protein significantly alters protein structure and function.[5]

Indeed, the mass and structure of PEG have been shown to play an important role in PEG conjugated protein delivery. For example, small PEGs are more rapidly cleared than larger ones from blood.[6-8] It has also been shown that the structure of PEG molecule markedly influenced PEG–protein conjugation.[9,10]

Despite the extensive investigations on PEG conjugated proteins, the effect of mass and PEG structure on the protein-polymer complexation is poorly understood. Therefore, the aim of this study was to evaluate the effects of both mass and structure of PEG polymers on the protein-polymer interactions.

β-Lactoglobulin (*β*-LG) is an abundant milk protein with the ability to bind a wide range of hydrophobic and hydrophilic compounds.[11-20] Under physiological conditions, *β*-LG exists as a mixture of monomers and dimers the equilibrium ratio of which depends on the association constant of the dimer and on the protein concentration. Each monomer consists of 162 amino acid residues and has a molecular mass of 18 kDa.[21,22] *β*-LG was used as a simple model protein, in order to provide a better understanding of how mass and

structure of PEG affect the polymer-protein interaction at the molecular level. In this study, we report the spectroscopic analysis, thermodynamic parameters, TEM and molecular modeling of the *β*-LG complexes with PEG-3000, PEG-6000 and mPEG-anthracene (**Scheme 1**), in aqueous solution at pH 7.4. The structural analysis, regarding protein binding sites and the effects of PEG hydrophilic and hydrophobic compositions on the *β*-LG stability and morphology is also reported here.

Experimental section

Materials

β-Lactoglobulin (A variant, purity > 90%), PEG-3000 and PEG-6000 were purchased from Sigma Chemical Company and used as supplied. Methoxypoly (ethylene glycol) anthracene (mPEG-anthracene) was from Polymer Source (Quebec). Other chemicals were of reagent grade and used without further purification.

Preparation of stock solutions

PEG-3000, PEG-6000 and mPEG-anthracene were dissolved in Tris-HCl solution (pH 7.4). The *β*-lactoglobulin was dissolved in aqueous solution (4 mg/ml to obtain 0.25 mM protein content) containing Tris-HCl (pH 7.4). The protein concentration was determined spectrophotometrically using the extinction coefficient of 17600 M^{-1} cm^{-1} at 280 nm.[23]

FTIR spectroscopic measurements

Infrared spectra were recorded on a FTIR spectrometer (Impact 420 model, Digilab), equipped with deuterated triglycine sulphate (DTGS) detector and KBr beam splitter, using AgBr windows. The solution of polymer was added dropwise to the protein solution with

constant stirring to ensure the formation of homogeneous solution and to reach the target polymer concentrations of 15, 30 and 60 μM with a final protein concentration of 60 μM. The detailed spectroscopic treatments were carried out according to previous reports.[14, 24]

Analysis of protein conformation

Analysis of the secondary structure of *β*-lactoglobulin and its PEG complexes was carried out using FTIR spectroscopic analysis based on literature reports.[14,25] The protein secondary structure is determined from the shape of the amide I band, located at 1660-1650 cm^{-1}. The FTIR spectra were smoothed and their baselines were corrected automatically using the built-in software of the spectrophotometer (OMNIC ver. 7.3). Thus, the root-mean square (rms) noise of every spectrum was calculated. By means of the second derivative in the spectral region 1700-1600 cm^{-1}, five major peaks for *β*-lactoglobulin and the complexes were resolved. The above spectral region was deconvoluted by the curve-fitting method with the Levenberg-Marquadt algorithm and the peaks related to *α*-helix (1660-1650 cm^{-1}), *β*-sheet (1640-1610 cm^{-1}), turn (1680-1660 cm^{-1}), and *β*-antiparallel (1692-1680 cm^{-1}) were adjusted and the area were measured with the Gaussian function. The area of all the component of the bands assigned to a given conformation were then summed up and divided by the total area. The curve fitting analysis was performed using the GRAMS/AI Version 7.01 software of the Galactic Industries Corporation.

Fluorescence spectroscopy

Fluorescence spectra were recorded with a Perkin-Elmer LS55 Spectrometer. The *β*-lactoglobulin fluorescence emission was recorded at λ_{ex} = 295 nm and λ_{em} 342 nm. Stock

solution of β-lactoglobulin (30 μM) in Tris-HCl buffer was prepared at 24 ± 1 °C. Samples containing 0.06 ml of the above protein solution and various polymer solutions were mixed to obtain final polymer concentrations, ranging from 15 to 45 μM with constant β-LG content (30 μM).

Transmission electron microscopy

The specimens were observed using a Philips EM 208S microscope operating at 180 kV. The morphology of the complexes of β-LG with PEG-3000 and mPEG-anthracene in aqueous solution at pH 7.4 were observed using transmission electron microscopy (TEM). One drop (5–10 μL) of the freshly-prepared mixture [β-lactoglobulin solution (60 μM) + polymer solution (60 μM)] in Tris-HCl buffer (24 ± 1 °C) was deposited onto a glow-discharged carbon-coated electron microscopy grid. The excess liquid was absorbed by a piece of filter paper and a drop of 2% uranyl acetate negative stain was added before drying at room temperature. The particle diameter was estimated by using IMAGEJ® software analysis of the TEM micrographs. It should be emphasized that our determination of the size was based on at least 5 groups (~1cm x 1cm of the TEM image), each containing almost 100 particles and the average size was deduced from these groups.

Molecular modeling

The docking studies were carried out with ArgusLab 4.0.1 software (Mark A. Thompson, Planaria Software LLC, Seattle, Wa, http://www.arguslab.com). The β-LG structures were obtained from literature report[22] and the PEG three dimensional structures were generated from PM3 semi-empirical calculations using Chem3D Ultra 11.0. The whole protein was selected as a potential binding site, since no prior knowledge of such site was available in

the literature. The docking runs were performed on the ArgusDock docking engine using regular precision with a maximum of 1000 candidate poses.

Results and Discussion

Fluorescence spectroscopy and binding parameters for polymer-*β*-LG adducts

The intrinsic fluorescence of *β*-LG was studied in the presence of various polymer concentrations, in order to determine the nature of interaction and the binding parameters between the PEG and the *β*-LG. The fluorescence emission spectra of *β*-LG (10 μM) at pH 7.4 with different concentrations of PEG-3000, PEG-6000 and mPEG-anthracene are shown in Fig. 1. The emission maxima (λ_{em}) of the free *β*-LG was observed at 342 nm. The fluorescence intensity of *β*-LG was gradually decreased as the polymers concentration increased (Fig. 1A-C). The changes indicate that the quenching of protein intrinsic fluorescence is due to polymer-protein complexation.[11,12] Furthermore, a minor blue shift (from 342 to 340 nm) was observed with increasing PEG concentration. This blue shift was more pronounced for mPEG-anthracene (from 342 to 338 nm). The blue shift indicates that the fluorophore (i.e., tryptophan) is experiencing a more hydrophobic environment as compared to its native state. This means protein in the presence of PEG undergoes a conformational change, such as that the tryptophan residue (fluorophore) inside *β*-LG becomes more exposed to the surface after the polymer-protein complex formation. This is also consistent with the FT-IR results that showed major protein conformational changes upon polymer interaction (will be discussed further on).

The fluorescence quenching of a protein by ligand can be dynamic, static or both.[26,27] To elucidate the nature of fluorescence quenching mechanism, the fluorescence data was analyzed using the Stern-Volmer equation (Eq. 1)

$$F_0/F = 1 + K_{SV}[Q] = 1 + K_q\tau_0[Q] \quad (1)$$

where, F_0 and F represent the steady-state fluorescence intensities in the absence and presence of quencher. K_q is the quenching rate constant, τ_0 is the average lifetime of protein in the absence of quencher (1.2 ns) for free β-LG at neutral pH.[12] [Q] is the molar concentration of quencher and K_{SV} is the Stern-volmer constant.[28] The plots of F_0/F versus [Q] showed a linear feature for all polymers (Fig. 2), which means that static or dynamic quenchings can occur.[26,27] The values of K_{SV} were obtained from the slope of linear regressions of the Stern-Volmer plots (Fig. 2) and the K_q values were deduced from equation 1 and listed in the Table 1. The K_q values for all PEG-β-LG complexes (at 298.15 K) were found to be greater than the maximum value for a diffusion-controlled quenching process (10^{10} M^{-1} s^{-1}),[29,30] which shows that the quenching mechanism of β-LG by PEG is static.

Additionally, the dynamic or static quenching can also be determined by temperature variations. In the case of dynamic quenching, higher temperature results in faster diffusion and consequently, in a larger quenching rate constant (K_q). In contrast, in static quenching, raising temperature results in decreasing complex stability and decreasing of the static quenching constant.[26,27] As shown in Table 1, the values of K_{SV} and K_q decreased with increasing temperature and this confirms that the static quenching is predominant in these PEG-protein complexes.

It should be noted that in the case of static quenching, the Stern-Volmer quenching constant (K_{SV}) can be taken as binding constant of the quencher to the fluorophore.[28-31] The calculated binding constant for PEG showed that PEG-3000 binds to *β*-LG with the binding affinities of the order 10^3 M^{-1} (Table 1). Increasing the PEG chain to PEG-6000 has no major effect on the affinities of PEG-*β*-LG binding (Table 1). However, by substitution of anthracene (a hydrophobic molecule) in PEG leads to a huge increase of K_{SV} value from 10^3 M^{-1} to 10^4 M^{-1} for mPEG-anthracene-*β*-LG adduct (Table 1). Therefore it is evident that the hydrophobic force plays an important role in the PEG-protein binding.

Thermodynamic analysis of polymer-*β*-LG adducts

The thermodynamic parameters were analyzed, in order to examine the different intermolecular forces involved in the formation of polymer- protein complexes with PEG-3000, PEG-6000 and mPEG-anthracene. The thermodynamic parameters (standard enthalpy changes, ΔH; standard entropy changes, ΔS and standard Gibbs free energy changes, ΔG) for PEG-protein interaction were determined at pH 7.4, conducted at three different temperatures: 298.15, 308.15 and 318.15 K, using the equations 2 and 3.

$$\log K_{SV} = \frac{-\Delta H}{2.303RT} + \frac{\Delta S}{2.303R} \quad (\mathbf{2})$$

$$\Delta G = \Delta H - T\Delta S \quad (\mathbf{3})$$

Where, T and R are the temperature and gas constants, respectively.

According to the binding constants K_{sv} measured at three temperatures (298.15, 308.15 and 318.15 K), the ΔH and ΔS values were estimated from the linear relationship between log K_{SV} and the reciprocal thermodynamic temperature (1/T) (Fig. 3 and Table 2). The ΔG was

calculated using Eq. (3). As one can see, the ΔH and ΔS were found to be -51.71 kJ.mol^{-1} and -98.58 J.mol^{-1} K^{-1} for the binding between PEG-3000 with β-LG and -33.21 kJ.mol^{-1} and -35.66 J.mol^{-1} K^{-1} for the binding between PEG-6000 with β-LG. While for mPEG-anthracene, the ΔH and ΔS were 11.63 kJ.mol^{-1} and 32.49 J.mol^{-1}.K^{-1} (Table 2). All three PEG-β-LG complexes have negative ΔH and ΔG, which show that the binding process was exothermic and spontaneous at different temperatures.

ΔS is a measure of the disorder in a system during the reaction and thus, in polymer-protein complex formation, ΔS involves in the two main processes with the opposite contributions: (i) the approaching of PEG to β-LG, which results in the decrease of freedom with negative ΔS and (ii) the binding of PEG to β-LG, which could lead to protein conformational changes increasing the freedom of the complex with positive ΔS. Therefore, the positive value of ΔS indicates that entropy provides a contribution to the standard Gibbs free energy changes (ΔG). Furthermore, the positive ΔS is frequently taken as a typical evidence for hydrophobic interaction.[32]

Interestingly, it is found that in the binding between PEG-3000 and PEG-6000 with β-LG, the major contribution to ΔG arises from the ΔH (negative value), rather than the ΔS (negative value), so the binding process is enthalpy driven (Table 2). Therefore, the negative ΔH and ΔS values (Table 2) suggest the involvement of van der Waals force and hydrogen bonding in the PEG-3000-β-LG and PEG-6000-β-LG complex formation.[33,34] However, a decrease in entropy (Table 2) is attributed to the formation of hydrogen bond between PEG-3000 and PEG-6000 with β-LG, which markedly reduces the degrees of freedom, because the system is more ordered after the complex formation. In contrast, the

binding reaction between mPEG-anthracene with *β*-LG, both ΔH (negative value) and ΔS (positive value) were favorable to a polymer-protein complexation (Table 2). However, the negative enthalpy (ΔH = -11.63 kJ.mol^{-1}) and entropy (T*ΔS = -9.68 kJ.mol^{-1} at 298.15 K) for mPEG-anthracene-*β*-LG, both terms provide about the same contribution to ΔG, which indicates that the binding process is enthalpy and entropy driven (Table 2). It can therefore be concluded that hydrogen bonding and hydrophobic interactions are the main forces behind the binding of mPEG-anthracene with *β*-LG.[35] These findings also suggest that PEG-protein complexation is more stable when both hydrogen bonding and hydrophobic contacts are involved in the binding process.

FT-IR spectroscopic analysis of polymer-*β*-LG complexes

The polymer-protein interaction was characterized by infrared spectroscopy. The protein amide I band at 1660-1650 cm^{-1} (C=O stretching vibrations) and amide II band at 1550-1530 cm^{-1} (C-N stretching coupled with N-H bending modes)[36] can be used to assess the polymer-protein complexation. The amide I band is also used to quantify protein conformational changes, upon ligand interaction.[14, 25]

Given that there was no major spectral shifting for the protein amide I and II bands upon polymer interaction, the difference spectra [(*β*-LG solution + polymer solution) – (*β*-LG solution)] were generated, in order to monitor the intensity variations of the amide bands and the results are shown in Fig. 4. At low polymer concentration 15 μM, several negative features were observed in the difference spectra for the protein amide I and amide II at 1642 and 1537 cm^{-1} (PEG-3000-*β*-LG), at 1640 and 1533 cm^{-1} (PEG-6000-*β*-LG) and at 1641 and 1538 cm^{-1} (mPEG-anthracene-*β*-LG) (Fig. 4A-C, diff., 15 μM). As polymer

concentration increased to 60 μM, larger negative features were observed for the protein amide I and amide II at 1640 and 1535 cm^{-1} (PEG-3000-*β*-LG), at 1639 and 1534 cm^{-1} (PEG-6000-*β*-LG) and at 1639 and 1538 cm^{-1} (mPEG-anthracene-*β*-LG), upon polymer-protein complexation (Fig. 4A-C, diff., 60 μM). These negative features are related to the intensity reduction of the protein amide I and amide II bands, upon polymer-protein complexation. The results indicate that the polymer-protein interaction occurs with protein C=O and C-N groups. It is worth mentioning that the observed decrease in intensity of the amide I and amide II in the presence of polymers is also due to a change in protein conformation, which is discussed below. This is also consistent with the fluorescence results that showed major protein conformational changes upon polymer interaction.

In order to evaluate the conformational changes of *β*-LG upon PEG interaction, a quantitative analysis of the protein secondary structure for the free *β*-LG and its complexes (*β*-LG-PEG) has been carried out and the results are shown in Figure 5 and Table 3. The free *β*-LG has 58% *β*-sheet (1640, 1623 cm^{-1}), 11% *α*-helix (1655 cm^{-1}), 14% turn structure (1667 cm^{-1}) and 17% *β*-antiparallel (1679 cm^{-1}) as previously reported.[14,18] Upon PEG interaction, major changes of the α-helix from 11% (free *β*-LG) to 34% (PEG-3000-*β*-LG), 28% (PEG-6000-*β*-LG) and 46% (mPEG-anthracene-*β*-LG) with a reduction of *β*-sheet structure from 58% (free *β*-LG) to 47% (PEG-3000-*β*-LG), 52% (PEG-6000-*β*-LG) and 29% (mPEG-anthracene-*β*-LG) were observed (Table 3). The major alterations of *β*-LG conformation (reduction of the *β*-sheet and increase of the *α*-helix structure) are due to a partial protein destabilization. Our results are consistent with those of the recent studies by CD spectroscopy that showed PEG-BSA interaction alters protein conformation.[37,38]

Morphological characteristics of polymer-*β*-LG aggregates

The changes in the morphological aggregation of *β*-LG molecules after polymer complexation can be observed visually by using transmission electron microscopy (TEM). The TEM photographs of *β*-LG in the absence and presence of PEG-3000 and mPEG-anthracene in aqueous solution at pH 7.4 are shown in Fig. 6. As TEM photograph of the native *β*-LG (i.e., without polymers Fig. 6A) shows, it is likely that we have minor spherical aggregates. Aggregates take the form of white masses due to the negative staining procedure employed. The observed changes in TEM photograph are consistent with the fact that as a globular protein, native *β*-LG is almost spherical with a packing density at the interior of the molecule, which shows that the hydrophobic amino acid residues tend to be buried inside the protein, whereas hydrophilic charged groups are located on the surface, in contact with the aqueous phase as reported in the literature.[39-41] The particle size analysis of *β*-LG in the absence of polymers shows that the particle size ranges from 3 to 12 nm with a mean diameter of 5.48 ± 2.29 nm (Fig. 6A).

Upon mixing *β*-LG with PEG-3000 and mPEG-anthracene, the stable dispersions of *β*-LG aggregates become more evident in the TEM photographs (Fig. 6B-C). These results suggest that PEG-protein complexation causes a major change in protein morphology. As a consequence, segments of different *β*-LG molecules may interact through hydrophobic contacts or by forming hydrogen bonds, leading to aggregation. TEM images show that the number and size of the spherical aggregate has been increased after PEG-*β*-LG complexes formed (Fig. 6B, C, E and F) compared to the small aggregate observed in native *β*-LG

molecules (Fig. 6A and 6D). The size aggregate analysis reveals that the mean diameter of the aggregation of *β*-LG with PEG-3000 and mPEG-anthracene is 12.09 and 17.57 nm, respectively (Fig. 6E). It is worth mentioning, that the increase of the diameters of *β*-LG aggregates are consistent with those of the binding constants estimated by fluorescence data that showed more stable complexes form with mPEG-anthracene (Table 1).

The results can be explained by the nature of the interactions between *β*-LG and PEG-polymers. As we mentioned earlier in the section related to the FT-IR and fluorescence spectroscopic studies, polymer induced major perturbations of secondary protein structure. The protein secondary structure is the specific geometric shape caused by intramolecular hydrogen bonding of amide groups. Therefore, in the case of PEG-3000-*β*-LG complex, the increases in diameter of *β*-LG aggregate (110%) is due to the intermolecular hydrogen bonding between PEG-3000 and protein, which constitutes the predominant interaction force of protein-polymer complexation, as shown by the thermodynamic analysis. Thus, intramolecular hydrogen bonds with amide groups are lost at the expense of the intermolecular hydrogen bonds between PEG and *β*-LG, which causes the changes in the secondary structure of protein and thereby their morphology. While, in the case of mPEG-anthracene-*β*-LG complex, 300% increase in *β*-LG aggregate diameter is due to the fact that hydrogen bonding and hydrophobic interactions are the main forces behind protein-polymer complexation. In native protein, this larger morphological perturbation comes from the fact that the hydrophobic amino acid residues are buried inside the protein core. Thus, to promote the hydrophobic interactions between mPEG-anthracene and *β*-LG, protein must expose its hydrophobic residues to the surface and adopt a conformation which facilitates

complex formation, thereby causing a larger perturbation in protein secondary structure than that of the PEG-3000 (Table 3).

Docking studies

Docking study was used to locate the preferred polymer binding sites with protein. The models of the docking for polymer are shown in Fig. 7 and Table 4. Several amino acids are located in the vicinity of PEG and PEG-anthracene (Fig. 7 and Table 4). The presence of several H-bonding systems stabilizes the PEG-*β*-LG and PEG-anthracene complexes (Table 4). As one can see different amino acids are involved in PEG and PEG-anthracene complexation, due to the mainly hydrophilic character of PEG and the very hydrophobic nature of PEG-anthracene. This is consistent with more stable complexation of mPEG-anthracene with *β*-LG than the PEG-3000 and the PEG-6000 (Table 1). The findings are also in agreement with the TEM results that showed larger increase in protein diameter with mPEG-anthracene than those of the PEG-3000 and the PEG-6000 (Fig. 6). Since *β*-LG contains a large hydrophobic domain it seems hydrophobicity of anthracene residue results in a stronger mPEG-anthracene-protein complex formation.

Conclusions

Spectroscopic results showed that PEG mass and compositions have a major effect on polymer-*β*-LG interactions. mPEG-anthracene forms more stable complexes than PEG-3000 and PEG-6000. Thermodynamic analysis showed that polymer-protein binding process is enthalpy and entropy driven with hydrogen bonding, van der Waals and hydrophobic contacts. Polymer-protein interaction alters *β*-LG conformation with mPEG-anthracene causing larger perturbations of protein conformation than PEG-3000 and PEG-

6000, due to its major hydrophobic character. Major alterations of protein morphology were observed as protein-PEG complexation occurred with drastic increase in the diameter of protein aggregates. Modeling showed the presence of several hydrogen bonding systems between PEG and different amino acids that stabilized polymer-*β*-LG complexes. The results are expected to provide important insight into the binding mechanism of protein with PEG and its derivatives and to increase our understanding about the effects of PEG on polymer-protein interactions.

Acknowledgements

The financial support of the Natural Sciences and Engineering Research Council of Canada (NSERC) is highly appreciated.

Note and references

1 K. Knop, R. Hoogenboom, D. Fischer and U.S. Schubert, *Angew. Chem. Int. Ed.*, 2010, **49,** 6288 – 6308.

2 Z. Cao and S. Jiang, *Nano Today,* 2012, **7,** 404-413.

3 A. Li H. P. Lehmann G. Sun, S. Samarajeewa, J.S. Zou, F. Zhang, M.J. Welch, Y. Liu and K. L. Wooley, ACS Nano, 2012, **10**, 8970-8982.

4 K. Kavitha and G.L. BhalaMurugan, *Int. J. Res. Pharm. Biomed. Sci.,* 2013, **4,** 296-304.

5 S. Jevševar, M. Kunstelj and V. G. Porekar, *Biotec. J.*, 2010, **5,** 113–128.

6 T. Yamaoka,Y. Tabata and Y. Ikada, *J. Pharm. Sci.*, 1994, **83**, 601–606.

7 S.J. DeNardo, Z. S. Yao, K.S. Lam, A.M. Song, P.A. Burke, G. R. Mirick, K.R. Lamborn, R. T. Donnell and G. L. DeNardo, *Clin. Cancer Res*. 2003, **9**, 3854S-3864S.

8 L. E. van Vlerken, K. Tushar, K. Vyas and M. M. Amij, *Pharm. Res.,* 2007, DOI: 10.1007/s11095-007-9284-6.

9 M. J. Roberts, M.D. Bentley and J. M. Harris, *Adv. Drug Deliv. Rev.,* 2002, **54,** 459-476.

10 H. Rachmawati, P. L. Febrina, R.A. Ningrum and D. S. Retnoningrum, *Int. J. Res. Pharm. Sci*., 2012, **3**, 228–233.

11 L. Liang, M. Subirade, *J. Phys. Chem. B***.** 2010, **114**, 6707-6712.

12 L. Liang, H.A. Tajmir-Riahi and M. Subirade, *Biomacromolecules*, 2008, **9**, 50-55.

13 X. Liu, L. Shang, S. Jiang, E. Dong, E. Wang, *Biophys. Chem*. 2006, **121**, 218-223.

14 J. Essemine, I. Hasni, R. Caprpentier, T.J. Thomas and H.A, Tajmir-Riahi, *Int. J. Biol. Macromol.,* 2011, **49**, 201-211.

15 G. Kontopidis, C. Holt and L. Sawyer, *J. Dairy Sci.,* 2004, **87**, 785-706.

16 G. Kontopidis, C. Holt and L. Sawyer, *J. Mol. Biol.,* 2002, **318**, 1043-1055.

17 D.C. Lange, R. Kothari, R.C. Patel and S.C. Patel, *Biophys. Chem,.* 1998, **74**, 45-51.

18 D. C. Kanakis, I. Hasni, P. Bourassa, P. Tarantilis, M.G. Polissiou and H.A. Tajmir-Riahi, *Food Chem.,* 2011, **127,** 1046-1055.

19 S. Brownlow, J.H.M. Cabral, R. Cooper, D. R. Flower, S. J. Yewdall, A.C.T. Polikarpov, L. Nort and L. Sawyer, *Structure*, 1997, **5,** 481-495.

20 F. Zsila, Z. Bikadi and M. Simonyi, *Biochem. Pharmacol.,* 2002, **64,** 1651-1660.

21 H.A. McKenzie and W. H. Sawyer, *Nature*, 1967**, 214***,* 1101-1104.

22 B.Y. Qin, M.C. Bewley, L. K. Creamer, H.M. Baker, E. N. Baker and G. B. Jameson, *Biochemistry,* 1998, **37,** 14014-14023.

23 M. D. Collini, L. Alfonso and G. Baldini, *Protein Science* 2000, **9,** 1968-1974.

24 F. Dousseau, M. Therrien and M. Pezolet, *Appl. Spectrosc.,* 1989, **43,** 538-542.

25 D. M. Byler H. Susi, *Biopolymers,* 1986, **25***,* 469-486.

26 S. Roufik, S. F. Gauthier, X. J. Leng and S. L. Turgeon, *Biomacromolecules,* 2006, **7**, 419–426.

27 A. Uttam, G. Subhadip, D. N. Kumar, G. Narayani and M. Ramakanta, *Indian J. Chem., Sect A*, 2013, **52**, 1031-1040.

28 J. R. Lakowicz,. Principles of fluorescence spectroscopy, 3nd ed. *Springer*, New York, 2006.

29 G. Zhang, Q. Que, J. Pan and J. Guo, *J. Mol. Struct.,* 2008, **881**, 132-138.

30 J. B. Xiao, X.Q. Chen and X. Y. Jiang, X. Y. M. Hilczer and M. Tachiya, *J. Fluoresc*., 2008, **18,** 671-678.

31 G. B. Behera, B.K. Mishra, P.K. Behera and M. Panda, *Adv Colloid Interfac*., 1999,

82:1-42.

32 P. D. Ross and S. Subramanian, *Biochemistry*. 1981, **20,** 3096–3102.

33 O.K. Abou-Zied and O.I. K. Al-Shihi, *J. Am. Chem. Soc*., 2008, **130,** 10793–10801.

34 Q. Zhou and T. M. Swager, *J. Am. Chem. Soc,*. 1995, 117,12593–12602.

35 J. Tian, S. Wei, Y. Zhao, R. Liu and S. Zhao, *J. Chem. Sci*., 2010, **132**, 391–400.

36 S. Krimm and J. Bandekar, *Adv. Protein Chem*., 1986, **38**,181-346.

37. S. Rawat, R. Suri, D. K. Sahoo, *Biochem. Biophys. Res. Commun*. 2010, **392**, 561-566.

38. V. Kumar, V. K. Sharma, D. S. Kalonia, *Int. J. Pharm*., 2009, **366**, 38-43.

39. E. Dickinson and P. Walstra (Eds.), Food Colloids and Polymers: Stability and Mechanical Properties, Royal Society of Chemistry, Cambridge, pp. 332–340, 1993, UK.

40. R. N. Z´u˜niga, A. Tolkach, U. Kulozik J. M. Aguilera, *J. Food Sci*., 2010, **75***,* E261-E268.

41. L. Bateman, A. Ye and H. Singh, *J. Agric. Food Chem.,* 2010, **58**, 9800-9808.

Captions for Figures

Figure 1. Fluorescence emission spectra of *β*-LG in 10 mM Tris-HCl (a) under varying concentrations of (**A**) PEG-3000, (**B**) PEG-6000 and (**C**) mPEG-anthracene. λ_{ex} = 295 nm. T= 298.15 K, pH 7.4, [*β*-LG] = 30 μM. Concentrations of polymers from (a) to (e) are 0, 15, 25, 35 and 45 μM, respectively.

Figure 2. Stern-Volmer plots for fluorescence quenching data of the PEG-3000-*β*-LG (**A**), PEG-6000-*β*-LG (**B**) and mPEG-anthracene-*β*-LG (**C**) at three different temperatures and pH 7.4.

Figure 3. van't Hoff plots of *β*-LG interaction with the three polymers; PEG-3000 (**A**), PEG-6000 (**B**) and mPEG-anthracene (**C**).

Figure 4. FTIR spectra in the region of 1800-600 cm^{-1} of hydrated films (pH 7.4) for free *β*-LG (60 μM) and its PEG complexes for (**A**) PEG-3000 and (**B**) PEG-6000 and (**C**) mPEG-anthracene with difference spectra (diff.) (bottom two curves) obtained at different polymer concentrations (indicated on the figure).

Figure 5. Second derivative resolution enhancement and curve-fitting of the amide I region (1700-1600 cm^{-1}) for free *β*-LG and its PEG complexes with 60 μM polymer (pH 7.4).

Figure 6. TEM photographs showing the morphology of *β*-LG at pH 7.4 and 24°C: (A) in the absence of the polymers; in the presence of the: (B) PEG-3000 and (C) mPEG-anthracene; The histogram of *β*-LG particle size distribution: (D) in the absence of the PEG;

in the presence of the: (E) PEG-3000, (F) mPEG-anthracene (the concentrations of *β*-LG and polymers were 60 μM in all samples).

Figure 7. Docking results of PEG–*β*-LG and PEG-anthracene-*β*-LG complexes. View of the nearest amino acids surrounding PEG with H-bonding network and free binding energy.

Table 1. The quenching constants for PEG-*β*-LG complexes at three different temperatures

Complexes	Temperature (K)	Quenching constants	
		Stern-Volmer constant, K_{SV} (M^{-1})	Quenching rate constant, K_q ($M^{-1}S^{-1}$)
PEG-3000-*β*-LG	298.15	9.2×10^3	7.67×10^{12}
	308.15	3.2×10^3	2.67×10^{12}
	318.15	2.5×10^3	2.08×10^{12}
PEG-6000-*β*-LG	298.15	9.7×10^3	8.08×10^{12}
	308.15	5.0×10^3	4.17×10^{12}
	318.15	4.2×10^3	3.5×10^{12}
mPEG-anthracene-*β*-LG	298.15	5.5×10^4	4.58×10^{13}
	308.15	4.5×10^4	3.75×10^{13}
	318.15	4.1×10^4	3.41×10^{13}

Table 2. Thermodynamic parameters for PEG-*β*-LG complexes and the nature of interaction predicted from these parameters

Complexes	Thermodynamic parameters			Predominant interaction
	ΔH (KJ. mol^{-1})	ΔS (J. mol^{-1}. K-1)	ΔG (KJ. mol^{-1})	
PEG-3000-*β*-LG	-51.71	-98.58	-22.32 (298.15K) -21.34 (308.15K) -20.35 (318.15K)	Van der Waals forces and hydrogen bonding
PEG-6000-*β*-LG	-33.21	-35.66	-22.57 (298.15K) -22.21 (308.15K) -21.86 (318.15K)	Van der Waals forces and hydrogen bonding
mPEG-anthracene-*β*-LG	-11.63	32.49	-21.31 (298.15K) -21.64 (308.15K) -22.96 (318.15K)	H-bonding and Hydrophobic interactions

Table 3: **Secondary structure analysis for amide I region (infrared) in free *β*-LG and its polymer complexes at pH 7.4.**

Amide I (cm^{-1}) components	free *β*-LG (%) 60 µM	PEG-3000 (%) 60 µM	PEG-6000 (%) 60 µM	mPEG-anthracene (%) 60 µM
α-helix (±2) 1654-1660	11	34	28	46
β-sheet (±2) 1614-1637	58	47	52	29
turn (±2) 1670-1678	14	12	12	18
β-antiparallel (±1) 1680-1691	17	7	8	7

Table 4. Amino acid residues involved in PEG-*β*-LG complexes

Complex	Amino acids in the vicinity of PEG	$\Delta G_{binding}$ (Kcal/mol)
PEG-*β*-LG	*Glu-44, Glu-45, **Lys-47, Glu-55, *Gln-59, **Gln-68, *Lys-70, Gln-159	- 5.57
PEG-Ant-*β*-LG	Leu-39, Val-41, Leu-58., Lys-60, Lys-69, Ile-71, **Asn-88, **Asn-90, Met-107, *Asn-109, Glu-114, Ser-116	- 10.79

***Hydrogen bonding involved with these amino acids.**

24

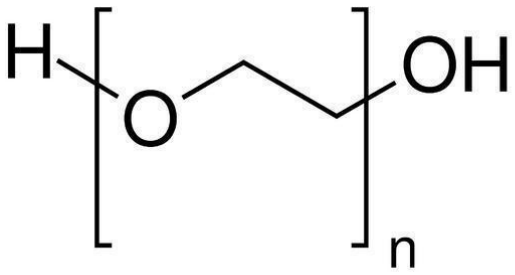

Poly(ethylene glycol) (PEG)

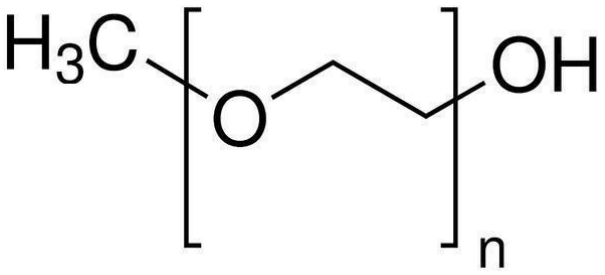

Methoxypolyethylene glycol (mPEG)

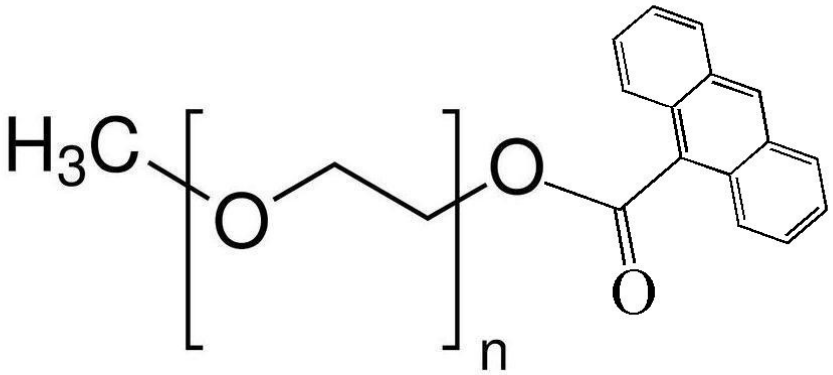

α-anthracene-terminated Methoxypolyethylene glycol (mPEG-anthracene)

Scheme 1

25

Figure 1

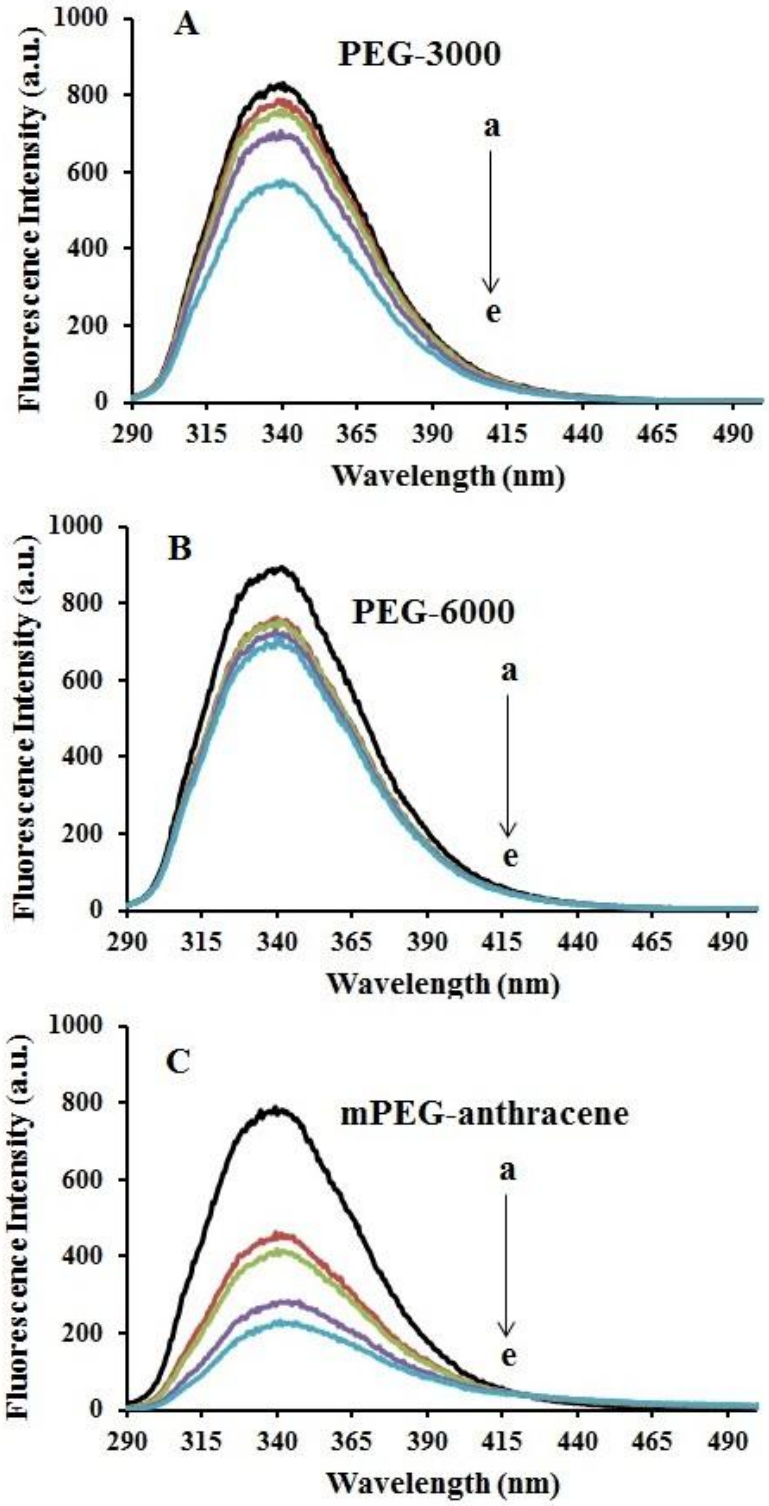

Figure 2

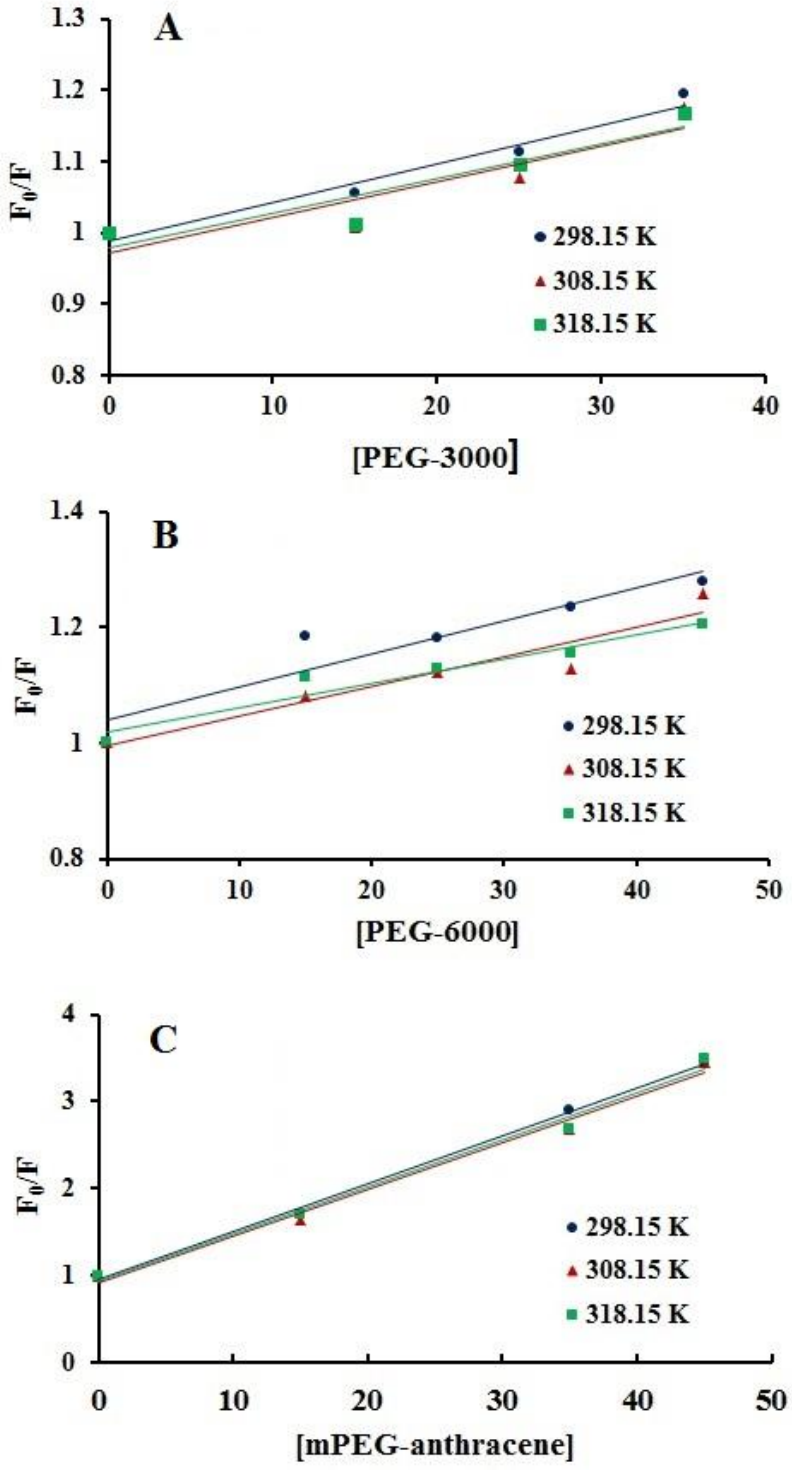

27

Figure 3

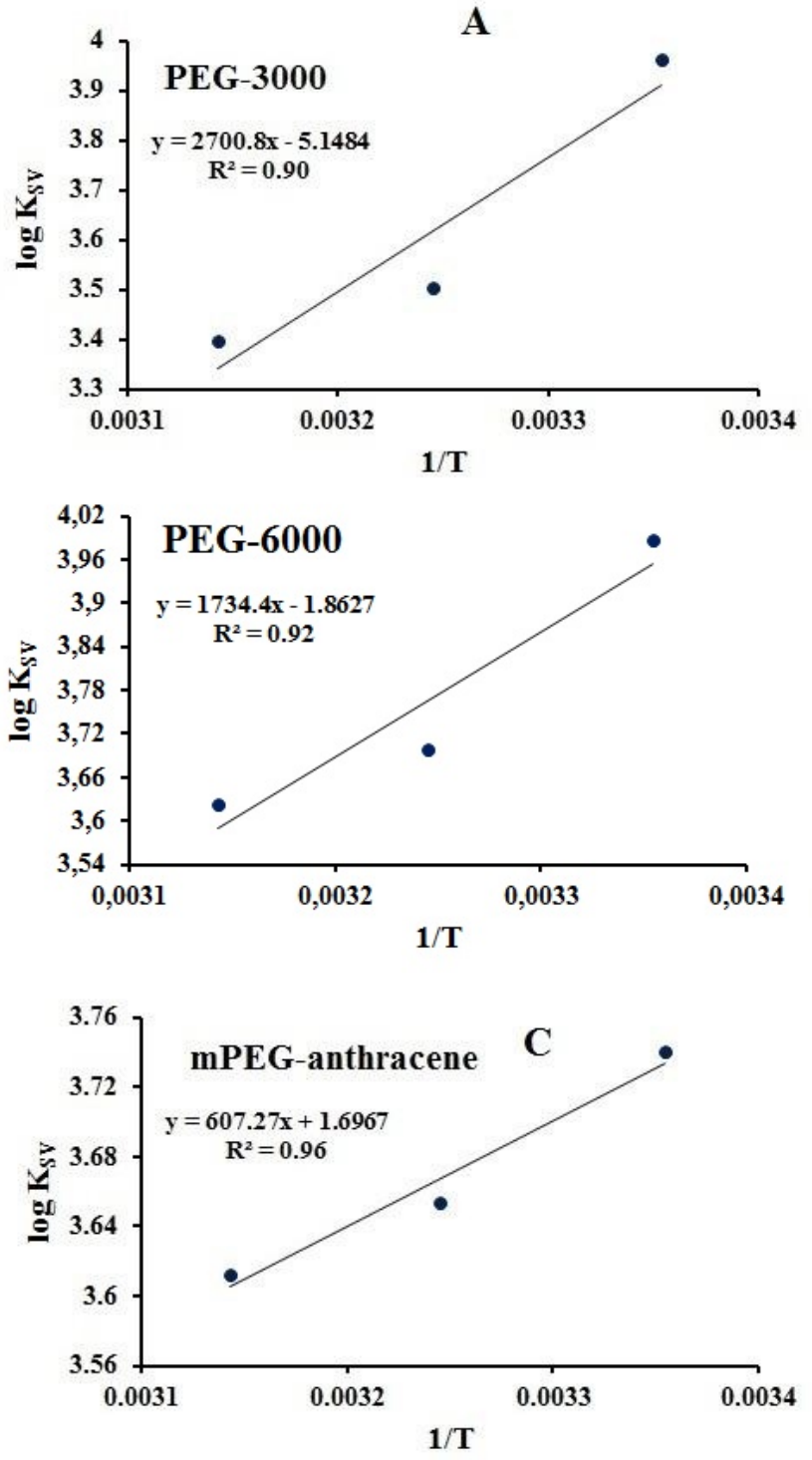

Figure 4

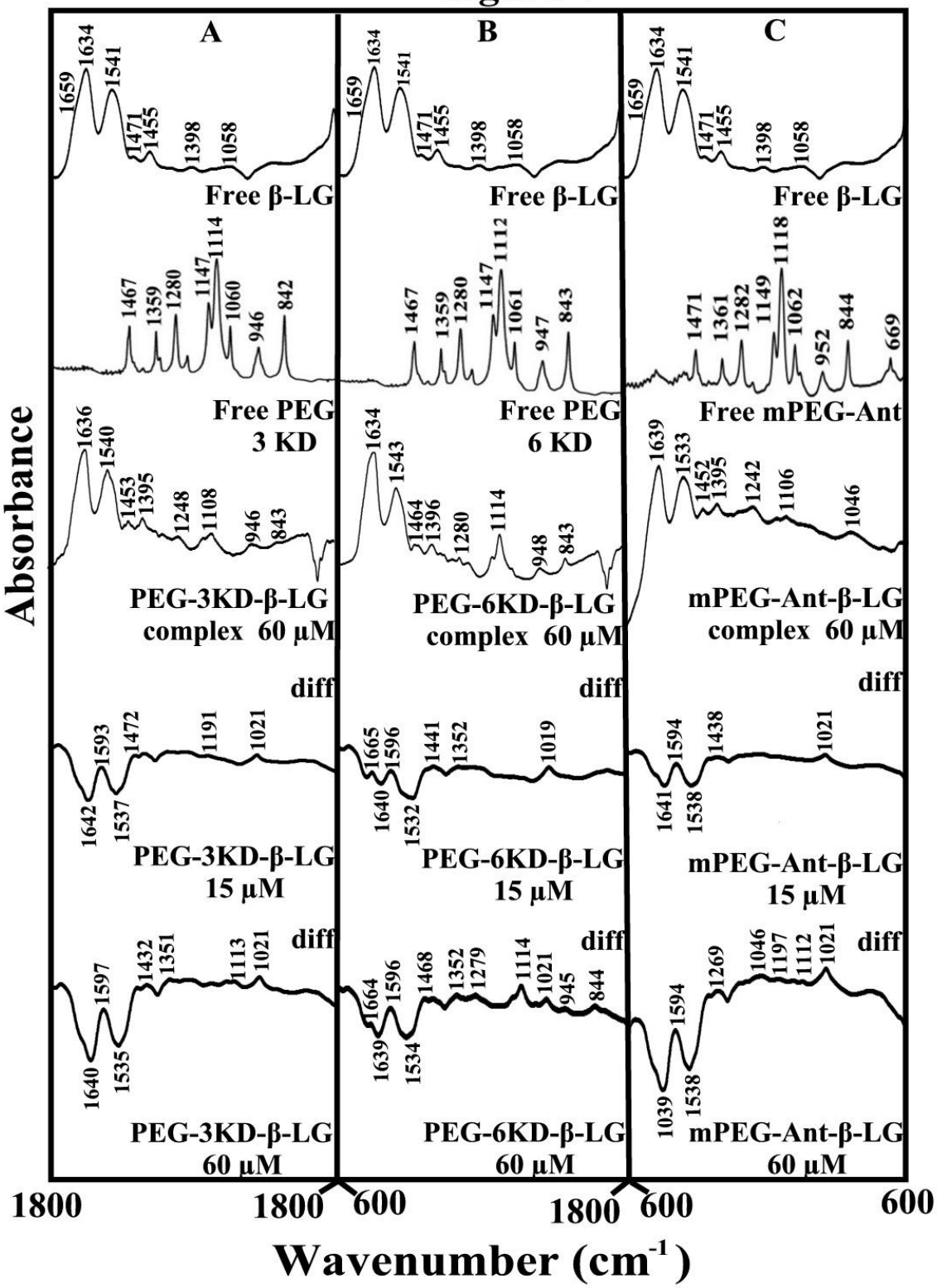

29

Figure 5

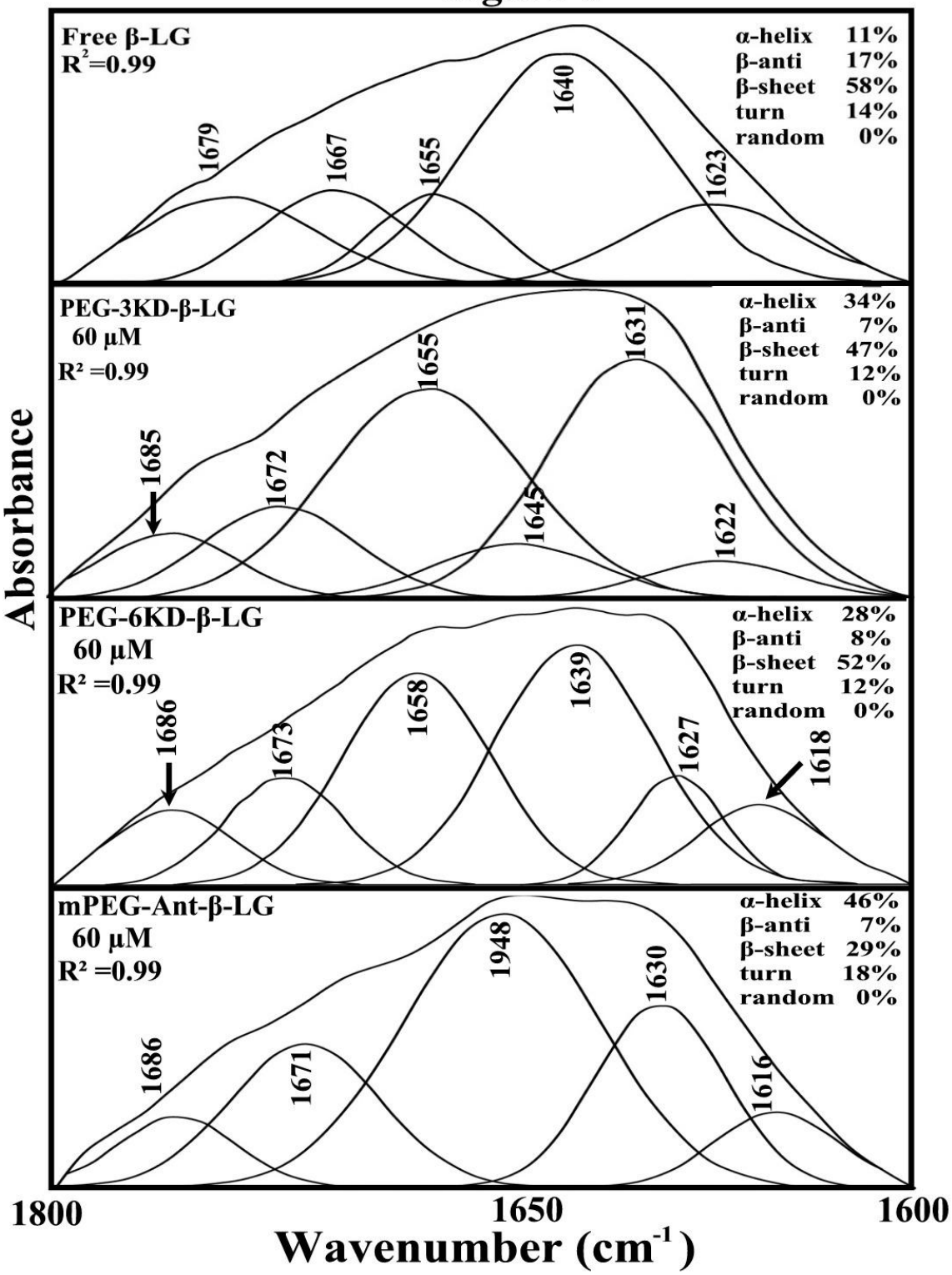

Figure 6

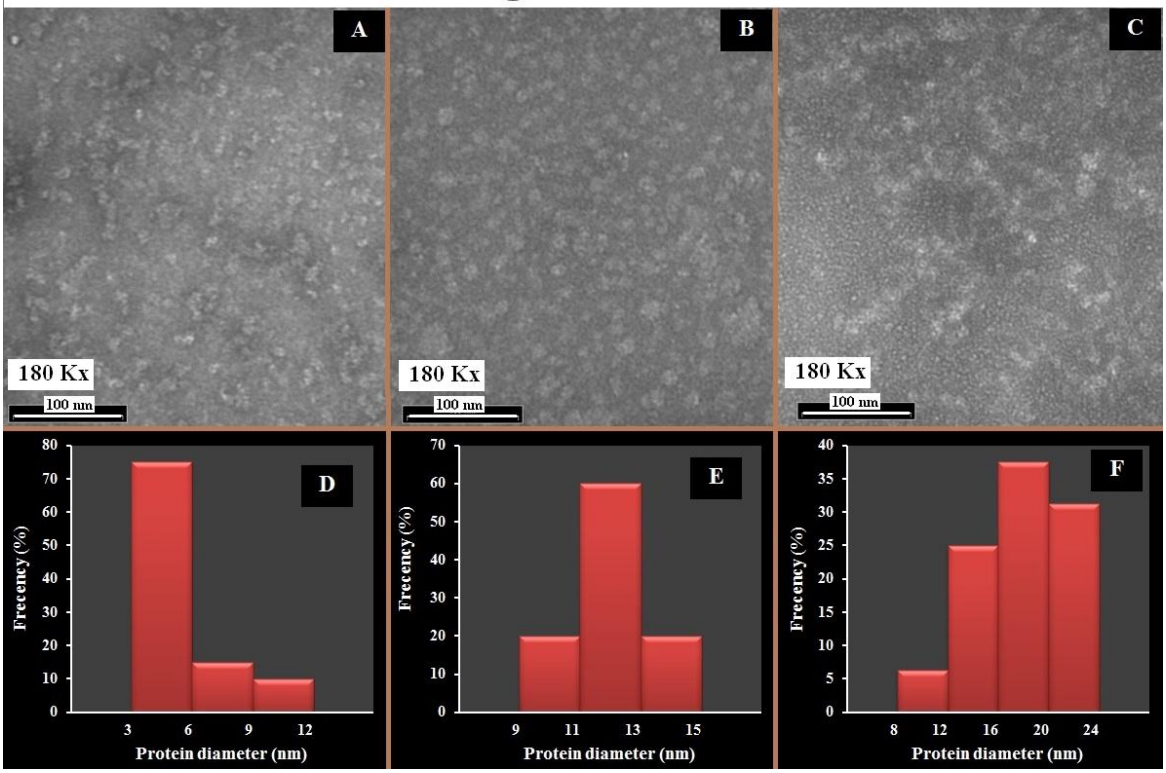

31

Figure 7